

EPR of Defects in Semiconductors: Past, Present, Future

© G.D. Watkins

Department of Physics, Lehigh University,
Bethlehem, PA 18015, USA

E-mail: gdw0@lehigh.edu

Important physical concepts learned from early EPR studies of defects in silicon are reviewed. Highlighted are the studies of shallow effective-mass-like donors and acceptors by Feher, of deep transition element impurities by Ludwig and Woodbury, and of vacancies and interstitials by Watkins et al. It is shown that the concepts learned in silicon translate remarkably well to the corresponding defects in the other elemental and compound semiconductors. The introduction over the intervening years of sensitive optical and electrical detection methods, and the recent progress in single defects detection insure the continued vital role of EPR in the future.

For over forty years, electron paramagnetic resonance (EPR) has played a key role in the study of point defects in semiconductors. Because of the detailed structural information available from the spectrum of a defect — symmetry from its angular dependence, and the atomic and lattice structure from its hyperfine interactions — it has proven to be uniquely able to identify a defect, to map out its wavefunction in the lattice, and determine its microscopic structure.

In this short presentation, I can present only a very few of the highlights, with apologies to the many, many EPR scientists who have made, and are continuing to make, vital contributions to our understanding of defects in semiconductors.

I. Past

1. Shallow Effective-Mass Impurities

Over forty years ago, Feher [1] introduced the important technique of electron-nuclear double resonance (ENDOR), where the nuclear resonance of nearby lattice atoms could be detected as a change in the EPR signal of a defect. With this, he was able for the first time to map out the wavefunction of the $S = 1/2$ bound electron of the shallow donor in silicon over the surrounding silicon lattice sites [2]. This served to establish in beautiful detail the correctness of the theory of Kohn and Luttinger [3], which described the wavefunction as a large orbit hydrogenic envelope function (effective-mass electron, dielectric shielded from the positive core) multiplying a sum of the free electron states at the conduction band valley minima.

The shallow acceptor in silicon was more difficult because, for it, the top of the valence band is at the Γ -point ($k = 0$), with orbital angular momentum $L = 1$, giving $J = 3/2$ for the bound hole. The hole is therefore strongly sensitive to random strains in the crystal and the acceptor resonance was too broad to detect. Feher solved the problem by applying uniaxial stress to the crystal, which lifted the degeneracy of the bound $J = 3/2$ hole and made the resonance observable [4], again confirming the general features of the Kohn-Luttinger theory. Twenty years later, with higher quality, lower internal strain crystals, Neubrand

was able to detect for the first time the acceptor resonance in the absence of external strain, and confirm the complete $J = 3/2$ spectrum for the bound hole [5].

This pioneering EPR work in silicon has served to set the pattern of understanding for all of the elemental and compound semiconductors. Similar shallow $S = 1/2$ effective-mass donor resonances have subsequently been observed in many of the semiconductors, but the shallow $J = 3/2$ acceptors have resisted detection, the valence band maximum being at $k = 0$ for all. The acceptors have been observed in a very few cases, but only again either when stress was externally applied to the cubic semiconductor, or when internally available for a few non-cubic semiconductors.

2. Deep Transition Element Impurities

At about the same time, Ludwig and Woodbury initiated a systematic study of the $3d$ transition element impurities in silicon, which continued through the 1960's [6]. Using EPR and ENDOR, several charge states of most of the $3d$ transition element impurities were observed and a simple physical picture of their properties emerged.

This is summarized in fig. 1. The sign of the crystal fields experienced by the d -electrons is reversed for the interstitial and substitutional sites. For the interstitial site, the crystal field can be considered to arise primarily from the positive cores of the four nearest silicon atoms, which are exposed because their charge compensating valence electrons are involved in bonds pointing away from the interstitial site. Therefore, as shown in the figure, the triply degenerate $d(t_2)$ orbitals are lower in energy because they interact more strongly with the neighbors than the doubly degenerate $d(e)$ orbitals, which better avoid them. In the substitutional site, the negative charge of the electrons in the bonds to the impurity dominate, and the level order is reversed.

Starting from the free ion $3d^\alpha 4s^\beta$ configuration for a particular charge state, all $\alpha + \beta$ electrons go into these orbitals for the non-bonding interstitial case, as expected. For the substitutional impurities, which require four electrons to complete their bonds to the four silicon neighbors, $\alpha + \beta - 4$ remain to go into the d -orbitals. In both cases, the levels are filled according to Hund's Rule, electrons

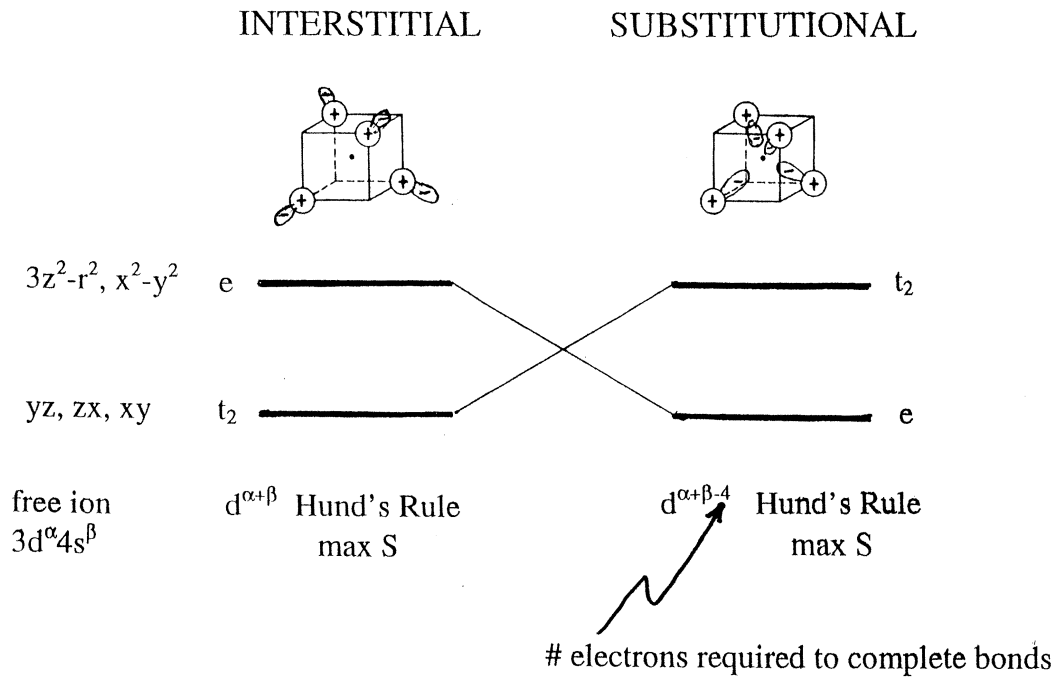


Figure 1. Simple crystal field model deduced for 3d transition element impurities in silicon [6].

paired (maximum S), first filling the lower level, spin-up, then the upper, spin-up, before filling, spin-down, in the lower, etc. The repulsive electron-electron interactions between the localized 3d orbitals, which force maximum spin, therefore dominate over the crystal field energy.

This general pattern, established very early for silicon, has been remarkably successful in interpreting the many subsequent EPR and optical results for transition elements in all of the semiconductors — elemental, III–V, and II–VI alike. In the compound semiconductors, the impurities tend to enter substitutionally on the metal sublattice. For them, the substitutional rules are the same as above, except that $\alpha + \beta - 3$ electrons go into the d -levels for the III–V's, the three electrons replacing now the three valence electrons associated with the neutral group-III atom that the impurity ion replaces. Similarly, for the II–VI's, the d -level occupancy number is $\alpha + \beta - 2$.

Of course, the excitement, and new physics, comes when departures are found, although there have been few so far. One interesting one is that of the shallow manganese acceptor in GaAs. In that case it has been found that Mn^0 is not d^4 , as expected by the simple rules above, but the Hund's rule d^5 , with a shallow bound hole [7]. Another departure has been found for substitutional Ni^- in silicon [8] and also for the corresponding d [7] substitutional ions of the 4d (Pd^-) and 5d (Pt^- , Au^0) series. For them, a Jahn-Teller distortion sets in, which overcomes the electron-electron coupling, giving $S = 1/2$ for their $e^4 t_2^3$ paramagnetic charge states. This anomaly has been explained as a result of strong charge transfer of the paramagnetic d -orbitals onto the four neighbors in the particular case of the transition elements at the end of each series [9].

3. Vacancies and Self-interstitials

Also, begun at about the same time, and continuing through the 1980's, I and my students have systematically probed the properties of the intrinsic defects — vacancies and self-interstitials — in silicon [10–12]. The approach taken was to produce the defects by 1–3 MeV electron irradiation in situ at cryogenic temperatures and to study by EPR the frozen-in isolated vacancies and interstitials, and then to warm up and study their migrational properties.

Fig. 2 summarizes the experiment and the overall pattern of results. Immediately after the irradiation, EPR of the isolated vacancy in two different charge states, V^+ and V^- , is observed. Long range migration of the vacancy with subsequent trapping by impurities occurs at ~ 70 K in n -type material, ~ 200 K in high resistivity material, and ~ 150 K in p -type material. As shown, a whole host of trapped vacancies have been identified by EPR, confirming unambiguously that the annealing is indeed the result of long range diffusion of the vacancy. Kinetic studies of the annealing have revealed the activation energies for vacancy diffusion as shown in the figure, along with the corresponding defects charge states. This was the first surprise. The high mobility well below room temperature, and its large dependence upon the vacancy charge state, were not anticipated.

A second surprise was the experimental observation that vacancy annealing can be stimulated even at 4.2 K by shining near bandgap light on the sample or by injecting electrons and holes electrically. This phenomenon, called recombination-enhanced migration, was also established to be occurring to a limited extent during the electron irradiation

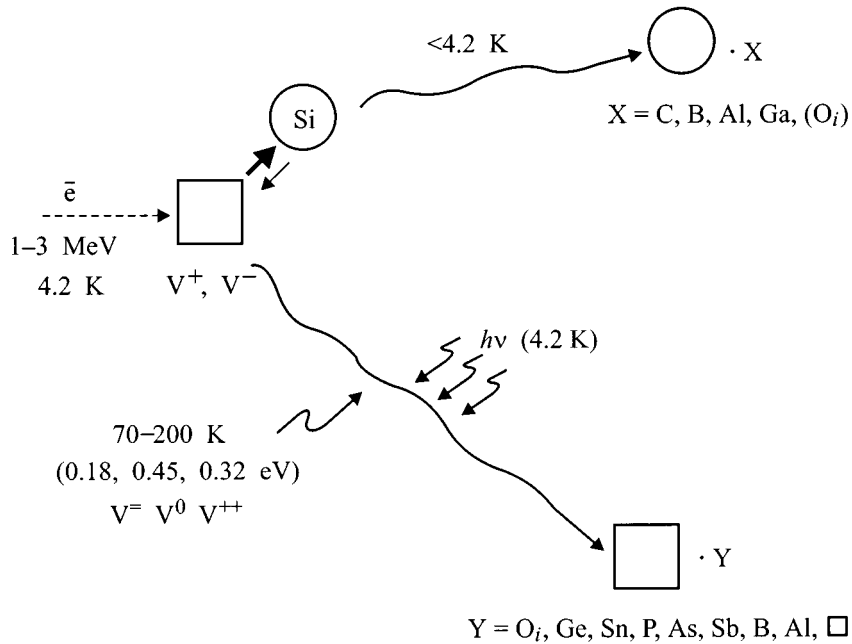


Figure 2. Evolution of events after a vacancy-interstitial pair is produced by an electron irradiation event in silicon [11,12].

itself, which also generates substantial electron-hole pair ionization.

A third even greater surprise was the observation, in the *p*-type material studied, that the interstitial had already migrated long distances during the initial electron irradiation at 4.2 K. Immediately after the irradiation, only interstitials trapped by impurities were observed, as illustrated in the figure, and in $\sim 1:1$ concentration to the isolated vacancies. Apparently, the interstitial is even more efficient in converting the capture of electrons and holes into the energy required for its migration.

Fig. 3 provides a simple interpretation of the electronic and lattice structure of the vacancy that has evolved from the EPR studies. Using the concept of simple molecular orbitals made up from the dangling bonds of the four vacancy neighbors, the various charge states can be understood by their successive population with the appropriate number of electrons, two for V^{++} , three for V^+ , etc. Here, the electron-electron interactions are weaker than in the transition element ion case, being spread mostly over the four nearest atom neighbors, but also onto their neighbors as well, and each level is filled before proceeding to the next. The interesting feature here is that Jahn-Teller energy-lowering distortions occurs as soon as partial occupancy of the degenerate t_2 orbital occurs. A tetragonal distortion occurs for V^+ , as observed in its EPR, because of its single occupancy in the t_2 orbital. A much larger tetragonal distortion occurs for V^0 being driven by the energy gain of two electrons in the orbital. For V^- , an additional dihedral distortion occurs.

These distortions turn out to have important consequences. For example, the increased two-electron Jahn-

Teller energy lowering for V^0 over the one-electron energy lowering for V^+ , actually serves to overcome the Coulomb repulsion between the two electrons and lower the vacancy first donor level ($0/+$) to a position, below the second donor level ($+/+$). This rare phenomenon, called negative- U , implies a net attraction between electrons at the vacancy. To account for this, the Jahn-Teller energy lowering for the vacancy single donor level ($0/+$) can be estimated to be at least ~ 0.5 eV [13]. With relaxation energies this large ($\sim 1/2$ the bandgap!), it is easy to understand how capture of electrons and holes at the vacancy can supply the necessary vibrational energy to overcome the small diffusion barriers indicated in fig. 2, and explain its athermal 4.2 K migration under electronic excitation.

Inspection of the wide variety of observed configurations for the trapped interstitials, combined with predictions of recent ab initio calculations for interstitial boron [14] and silicon [15,16] has served to suggest a similar simple physical picture for predicting the properties of such interstitials. Consider the *s* and *p* valence orbitals for the interstitial atom when placed in the high symmetry T_d interstitial position of the lattice. Populate them in the normal atomic order with electrons appropriate for the charge state of the interstitial. For $B_i^+(2s^2)$, $Al_i^{++}(3s^1)$ and $Si_i^{++}(3s^2)$, there is no orbital degeneracy, therefore no Jahn-Teller distortion, and the interstitial should stay on-center, as indeed observed for Al_i^{++} , and predicted by theory for the other two. For $B_i^0(2s^2 2p)$, $C_i^+(2s^2 2p)$, $Si_i^+(3s^2 3p^1)$, and their further degenerate *p*-level occupancy charge states, off-center Jahn-Teller distortions should occur into symmetry lowering bonding configurations, as indeed observed for B_i^0 and $C_i^{+,0,-}$, and predicted for all three atoms. Considering

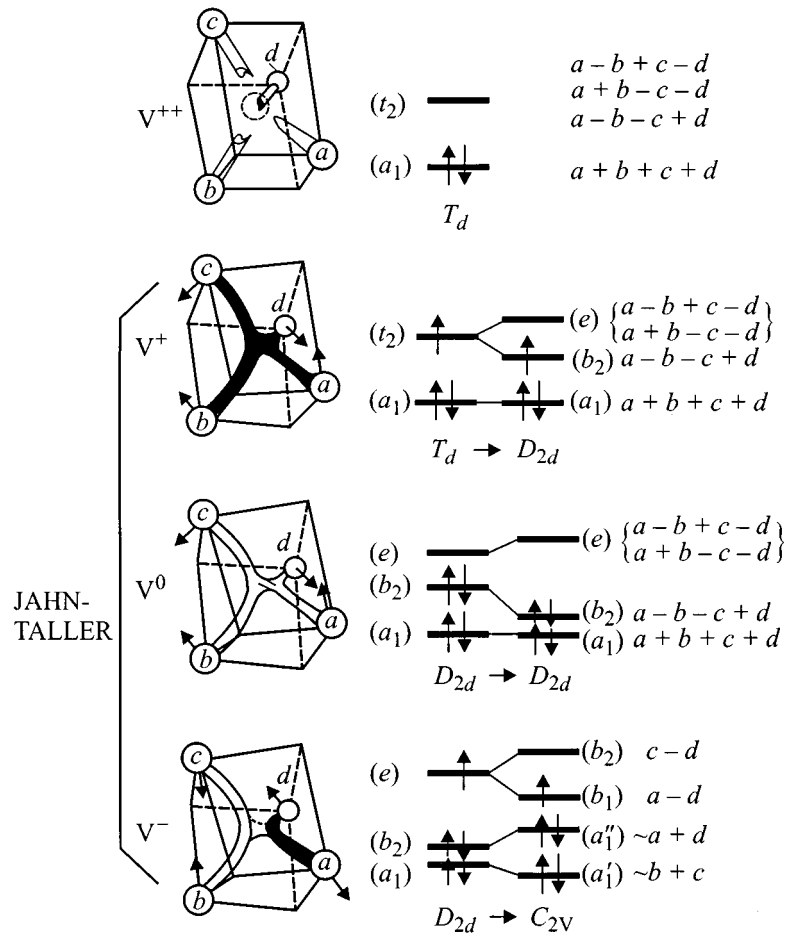


Figure 3. Simple one-electron model for the various charge states of the vacancy in silicon.

the large energies involved in p -bonding, it is again easy to understand efficient recombination-enhanced migration for the interstitial as it cycles back and forth between its various configurations during electron and hole capture.

Remarkably, therefore, the electronic and lattice structures for vacancies and interstitials in silicon can be understood in almost identical fashion, as summarized in fig. 4. In each case, there is a non-degenerate (a_1, s) level lowest and a three-fold degenerate (t_2, p) level higher, which are filled by the electrons appropriate for the charge state of the defect. Each level is filled before going to the next, and when orbital degeneracy results, symmetry-lowering Jahn-Teller distortions occur as bond reconstructions, rebonding configurations, etc.

The one-electron orbital pictures for vacancies and interstitials in fig. 4. must of course be generally applicable to all semiconductors — a vacancy always produces four dangling bonds, an interstitial in the undistorted tetrahedral site is always an ion surrounded by four non-bonding neighbors. In the II–VI semiconductors, for example, it provides a natural explanation for the on-center character observed by EPR for the chalcogen vacancies, $V_{VI}^+(a_1^1)$, and the trigonally distorted metal vacancies, $V_{II}^-(a_1^2 t_2^5)$ [11]. In ZnSe, the interstitial

$Zn_i^+(s^1)$, has also been observed, and is on-center, as predicted [11]. For the many other semiconductors about which no clear experimental defect identifications exist, these models may provide useful predictive properties, which, incidentally, provide a remarkable consistent simple physical

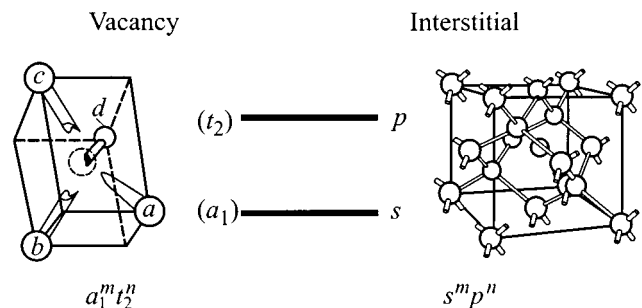


Figure 4. An identical simple one-electron orbital model appears to work for both vacancy and interstitial in silicon, the levels being filled, first the lower non-degenerate one, then the higher 3-fold degenerate one. When partial occupancy of the degenerate (t_2, p) orbitals results, $0 < n < 5$, large Jahn-Teller relaxations occur. Such a model should apply for all semiconductors.

explanation for the large lattice configurational changes currently often being predicted in modern state-of-the-art *ab initio* theoretical calculations. However, a word of caution is in order. It can also be considered to work for the only other identified intrinsic defects, V_{Ga}^0 in GaP [17], V_{C}^- in diamond [18] and V_{Si}^- in 3C-SiC [19]. However, there is an important difference. For their $a_1^2 t_2^3$ configuration, Hund's rule occupancy dominates, giving a non-degenerate $S = 3/2$ half-filled t_2 shell with no degeneracy and full undistorted T_d symmetry. Apparently, in these wider bandgap materials, with more localized vacancy orbitals, the electron-electron interactions are beginning to dominate. We may expect interesting surprises, therefore, as we are beginning to probe the intrinsic defects in these materials. Theorists, who do not so far have the ability to properly include these multiplet effects, must also beware.

II. Present and Future

Intensive EPR studies continue today and will in the future, particularly in probing defects in the wide bandgap semiconductors of high current interest today for visible/UV light emitting and high temperature electronic applications. To the arsenal of conventional EPR and ENDOR techniques discussed above have been added the powerful and greatly increased sensitivity optical and electrical detection methods. For example, the only EPR detection of an isolated interstitial in any semiconductor has been that of the zinc interstitial in ZnSe, performed by optical detection methods [20,21]. Here at the Ioffe Institute, important studies using the optical methods have been carried out in the groups of Romanov and Baranov, and much of the pioneering studies of electrical detection have been made by Vlasenko. In addition, a great deal of excitement is currently centered on the possibility of combining some of the various microscopic scanning techniques (optical, STM, AFM, magnetic cantilever) with the increased sensitivity EPR techniques to spatially resolve single defects. Promising recent success in this regard has been reported by et Gruber et al [22]. Using optical confocal microscopy, they have resolved and optically detected single isolated nitrogen-vacancy pair defects in diamond.

EPR will always remain a uniquely powerful tool for defect identification and electronic and lattice structure determination. As new semiconducting materials and device structures emerge in the future, it will therefore continue to play a vital role, particularly as promising new and more sensitive techniques for its detection evolve.

Acknowledgments

Support for the preparation of this review was provided by the National Science Foundation under Grant N DMR-92-094114, and the U.S. Navy Office of Naval Research (Electronic and Solid State Sciences Program) under Grant N N00014-94-1-0117.

References

- [1] G. Feher. Phys. Rev. **103**, 834 (1956).
- [2] G. Feher. Phys. Rev. **114**, 1219 (1959).
- [3] W. Kohn, J.M. Luttinger. Phys. Rev. **97**, 1721 (1955); *ibid.* **98**, 915 (1955).
- [4] G. Feher, J.C. Hensel, E.A. Gere. Phys. Rev. Lett. **5**, 309 (1960).
- [5] H. Neubrand. Phys. Stat. Sol. (b) **86**, 269 (1978).
- [6] G.W. Ludwig, H.H. Woodbury. In: Solid State Physics. Vol. 13 / Ed. by F. Seitz and D. Turnbull. Academic Press, N.Y. (1962). P. 223.
- [7] J. Schneider, U. Kaufmann, W. Wilkening, M. Baeumler, F. Köhl. Phys. Rev. Lett. **59**, 240 (1987).
- [8] L.S. Vlasenko, N.T. Son, A.B. van Oosten, C.A.J. Ammerlaan, A.A. Lebedev, E.S. Tapygov, V.A. Khramtsov. Sol. Stat. Commun. **73**, 393 (1990).
- [9] G.D. Watkins, P.M. Williams. Phys. Rev. **B52**, 16 575 (1995).
- [10] G.D. Watkins. In: Deep Centers in Semiconductors / Ed. by S. Pantelides. Gordon and Breach, N.Y. (1986). Ch. 3. (This provides a detailed description of the properties of the vacancy in silicon.)
- [11] G.D. Watkins. In: Electronic Structure and Properties of Semiconductors / Ed. by W. Schröter. Materials Science and Technology. Vol. 4. VCH, Weinheim (1991). Ch. 4. (This includes a review of vacancies and interstitials in all semiconductors.)
- [12] G.D. Watkins. In: Defects and Diffusion in Silicon Processing / Ed. by T.D. de la Rubia, S. Coffa, P.A. Stolk, C.S. Rafferty. MRS Symp. Proc. Vol. 469. Pittsburgh (1997). P. 139. (This is a concise review of vacancies and interstitials in silicon.)
- [13] G.A. Baraff, E.O. Kane, M. Schlüter. Phys. Rev. **B21**, 3563 (1980).
- [14] E. Tarnow. Europhys. Lett. **16**, 449 (1991).
- [15] R. Car, P.J. Kelly, A. Oshiyama, S.T. Pantelides. In: 13th Conf. Def. Semicond. / Ed. by L.C. Kimeling and J.M. Parsey, Jr., Metallurgical Soc. of AIME, Warrendale (1985). P. 269.
- [16] Y. Bar-Yam, J.D. Joannopoulos. In: 13th Conf. Def. Semicond. / Ed. by L.C. Kimeling and J.M. Parsey, Jr., Metallurgical Soc. of AIME, Warrendale (1985). P. 261.
- [17] T.A. Kennedy, N.D. Wilsey, J.J. Krebs, G.H. Strauss. Phys. Rev. Lett. **50**, 1281 (1983).
- [18] J. Isoya, H. Kanda, Y. Uchida, S.C. Lawson, S. Yamasaki, H. Itoh, Y. Morita. Phys. Rev. **B45**, 1436 (1992).
- [19] H. Itoh, M. Yoshikawa, I. Nashiyama, E. Sakuma. IEEE Trans. **NS37**, 1732 (1990).
- [20] F. Rong, G.D. Watkins. Phys. Rev. Lett. **58**, 1486 (1987).
- [21] K.H. Chow, G.D. Watkins. Phys. Rev. Lett. **81**, 2084 (1998).
- [22] A. Gruber, A. Dräbenstedt, C. Tietz, L. Fleury, J. Wrachtrup, C. von Borzyskowski. Science **276**, 2012 (1997).